



PREPRINT  
11-05  
AIAA CASE I  
(REVISED)

**AIAA 2000-1327**  
**Flexible Wing Model for Structural Sizing and Multidisciplinary Design Optimization of a Strut-Braced Wing**

F.H. Gern, A.H. Naghshineh-Pour,  
E. Sulaeman, R.K. Kapania  
Virginia Polytechnic Institute and State  
University, Blacksburg, VA  
and  
R.T. Haftka  
University of Florida,  
Gainesville, FL

**41st AIAA/ASME/ASCE/AHS/ASC  
Structures, Structural Dynamics  
and Materials Meeting & Exhibit**  
3-6 April 2000 / Atlanta, GA

# FLEXIBLE WING MODEL FOR STRUCTURAL WING SIZING AND MULTIDISCIPLINARY DESIGN OPTIMIZATION OF A STRUT-BRACED WING

Frank H. Gern<sup>\*</sup>, Amir H. Naghshineh-Pour<sup>†</sup>, Erwin Sulaeman<sup>‡</sup>, and Rakesh K. Kapania<sup>¶</sup>

*Department of Aerospace and Ocean Engineering  
Virginia Polytechnic Institute and State University  
Blacksburg, VA 24061-0203*

Raphael T. Haftka<sup>§</sup>

*Department of Aerospace Engineering, Mechanical and Engineering Sciences  
University of Florida  
Gainesville, FL 32611-6250*

## Abstract

This paper describes a structural and aeroelastic model for wing sizing and weight calculation of a strut-braced wing. The wing weight is calculated using a newly developed structural weight analysis module considering the special nature of strut-braced wings. A specially developed aeroelastic model enables one to consider wing flexibility and spanload redistribution during in-flight maneuvers. The structural model uses a hexagonal wing-box featuring skin panels, stringers, and spar caps, whereas the aerodynamics part employs a linearized transonic vortex lattice method. Thus, the wing weight may be calculated from the rigid or flexible wing spanload.

The calculations reveal the significant influence of the strut on the bending material weight of the wing. The use of a strut enables one to design a wing with thin airfoils without weight penalty. The strut also influences wing spanload and deformations. Weight savings are not only possible by calculation and iterative resizing of the wing structure according to the actual design loads. Moreover, as an advantage over the cantilever wing, employment of the strut twist moment for further load alleviation leads to increased savings in structural weight.

## Nomenclature

$AR$	wing aspect ratio
$b$	wing span
$c$	wing chord

<sup>\*</sup> Research Associate, Member AIAA

<sup>†</sup> Graduate Student, Student Member AIAA

<sup>‡</sup> Graduate Student

<sup>¶</sup> Professor, Associate Fellow AIAA

<sup>§</sup> Distinguished Professor, Fellow AIAA

Copyright © 2000 by the authors. Published by the American Institute of Aeronautics and Astronautics, Inc. with permission.

$c_B$	wing-box chord
$F_{sv}$	vertical strut force (z-direction)
$F_{sh}$	horizontal strut force (y-direction)
$L_{off}$	strut vertical offset length
$M_\infty$	freestream Mach number
$M(y)$	bending moment
$q_i(y)$	local lift distribution for element $i$
$s$	wing-strut intersection (from wing root)
$u$	unit step function
$u_{ab}, v_{ab}, w_{ab}$	backwash, sidewash and downwash velocity, respectively
$V(y)$	shear force
$w$	bending deflection
$W_e$	engine weight
$y_e$	spanwise engine position (from root)
$y$	spanwise coordinate
$\alpha, \beta$	lift coefficients at structural nodes
$\Lambda$	wing sweep angle
$\theta$	bending slope
$\Gamma$	vortex strength

## Introduction

Strut-braced wing configurations have been used both in the early days of aviation and today's small airplanes. Adopting thin airfoil sections required external structural wing support to sustain the aerodynamic loads. However, external structures cause a significant drag penalty. Gradually, it was understood that the external bracing could be removed and lower drag could be achieved by replacing the wing-bracing structure with a cantilever wing with an appropriate wing-box and thickness to chord ratios.

However, along with the idea of the cantilever wing configuration with its aerodynamic advantages, the concept of the truss-braced wing configuration

also survived. This is due to the tireless efforts of Werner Pfenninger at Northrop in the early 1950's [1] and his continuation of these efforts until the late 1980's. Using a strut or a truss offers the opportunity to increase the wing aspect ratio and to decrease the induced drag significantly without wing weight penalties relative to a cantilever wing. Also, a lower wing thickness becomes feasible reducing transonic wave drag and hence resulting in a lower wing sweep. Reduced wing sweep and high aspect ratios produce natural laminar flow due to low Reynolds numbers. Consequently, a significant increase in the overall aircraft performance is achieved [2], [3].

A number of strut-braced wing aircraft configurations have been investigated in the past. In continuing Pfenninger's work, Kulfan and Vachal from the Boeing Company performed preliminary design studies and evaluated the performance of a large subsonic military airplane [4]. They compared performance and economics of a cantilever wing with a strut-braced wing configuration. Two load conditions, a 2.5g maneuver and 1.67 taxi bump were used to perform structural analyses. Their optimization and sensitivity analyses showed that high aspect ratio wings with low thickness to chord ratios would result in a significant fuel consumption reduction.

For the cantilever configuration, a ground strike problem arose during taxiing. This issue was resolved by adding a strut to the wing structure. Moreover, the analysis indicated that the strut-braced wing configuration requires less fuel (1.6%), and results in lower takeoff gross weight (1.8%) and lower empty weight (3%) compared to the cantilever wing configuration. Cost comparisons showed that the operating costs of the strut-braced wing configuration were slightly less than those of the cantilever wing configuration because of a lower takeoff gross weight.

Park from the Boeing Company compared the block fuel consumption of a strutted wing versus a cantilever wing [5]. Even though he concluded that the use of a strut saves structural wing weight, the significant increase in the strut  $t/c$  to cope with its buckling at the -1.0g load condition increased the strut drag and hence did not appear practical for this transport aircraft due to a higher fuel consumption compared to the cantilever case.

Another study on strut-braced wing configurations was conducted by Turriziani et al. [6]. They addressed fuel efficiency advantages of a strut-braced wing business jet employing an aspect ratio of 25 over an equivalent conventional wing business jet with the

same payload range. They concluded that the strut-braced wing configuration reduces the total aircraft weight, even though wing and strut weight increased compared to the cantilever wing case, which is due to aerodynamic advantages of high aspect ratio wings. Furthermore, the results showed a fuel weight savings of 20%.

The strut-braced wing concept offers the possibility to reduce wing thickness without the penalty of an increased structural weight by reducing the bending moment on the wing. However, reduced wing thickness together with shorter wing chords result in smaller wing-box dimensions, thus significantly reducing wing-box torsional stiffness and rendering the wing more sensitive to aeroelastic problems like increased static aeroelastic deformation or reduced flutter and divergence speeds. The present approach highlights a possibility to remedy the problem of increased aeroelastic deformations by employment of the strut moment induced on the wing.

Previously investigated strut-braced wing concepts considered the strut to be rigidly attached to the wing. Therefore, strut buckling during negative g maneuvers was a major design issue, rendering the strut very heavy in order to overcome this buckling constraint [4], [5]. To avoid strut buckling, the present approach offers an innovative concept. A telescoping sleeve mechanism is employed to have the strut active only during positive g maneuvers. For negative g maneuvers, the wing acts like a cantilever wing, rendering the strut buckling constraint unnecessary. Furthermore, this arrangement allows one to apply a defined strut force at the 2.5g maneuver design load instead of the statically indeterminate one obtained from a rigid strut attachment. This way, the strut force as well as strut position can be optimized in order to achieve the maximum benefits out of the design concept.

To fully exploit the synergism from the strut-braced wing concept, an MDO approach has been chosen for aircraft design optimization. The multidisciplinary team consists of aerodynamics, structures, and a detailed investigation of interference drag. The aerodynamic analysis uses simple models for induced drag, parasite drag, and interference drag. All analyses are linked together, and the performance of the strut-braced wing aircraft is then optimized for minimum take-off-gross weight [3],[7],[8].

The MDO approach has been implemented in several aircraft designs. Grossman et al. [9]

investigated the interaction of aerodynamic and structural design of a composite sailplane subject to aeroelastic, structural, and aerodynamic constraints to increase the overall performance. They showed that the multidisciplinary design can yield results superior to the ones obtained from the sequential method. Another example is the application of MDO to a High Speed Civil Transport (HSCT). A significant effort has been made at the Multidisciplinary Analysis and Design (MAD) center of Virginia Tech to perform MDO of an HSCT. Several methods were developed for the better use of the MDO approach for aircraft conceptual and preliminary design. More information about this work can be obtained from [10] and [11].

The presented wing sizing module provides two essential features within the MDO environment. First, it is used to calculate the structural wing weight, i.e. the bending material weight of the wing-box. It has been found that commonly available wing weight calculation routines like the NASA Langley developed Flight Optimization System (FLOPS) [12] are not accurate enough for the present approach. Therefore, a program has been developed to accurately calculate the bending material weight of the wing based on a double plate model. The non-structural wing weight like flaps, slats, spoilers, ribs etc. is still calculated from the FLOPS equations by replacing the FLOPS bending material weight by the actual one.

Second, the wing sizing module features an idealized hexagonal wing-box model which has been provided for the project by Lockheed Martin Aeronautical Systems in Marietta, Georgia. The hexagonal wing-box permits accurate computation of the wing's torsional stiffness, therefore enabling one to investigate aeroelastic effects like static aeroelastic deformation, maneuver load alleviation, and to use flexible spanload distributions as design loads. As a result, the model can be employed to resize the wing according to the actual in-flight maneuver loads. This procedure usually leads to significant wing weight reductions.

### **Structural Wing Modeling**

Due to the unconventional nature of the proposed wing concept, commonly available weight calculation models for transport aircraft (such as the NASA Langley developed Flight Optimization System FLOPS [12]) are not accurate enough. A special bending weight calculation procedure was thus developed, taking into account the influence of the strut upon the structural wing design. In addition to the

strut design, a vertical strut offset was considered as to achieve a significant reduction in wing/strut interference drag.

### **Load Cases**

To determine the bending material weight of the strut-braced wing, two maneuver load conditions (2.5g maneuver, -1.0g pushover) and a taxi bump (-1.0g) are considered to be design critical. For the -1.0g pushover and for the -2.0g taxi bump, the strut is not active and the wing acts like a cantilever beam. Since the strut is not supporting the wing in these cases, very high deflections of the wing are expected for the -2.0g taxi bump. As a result, an optimization procedure is implemented to distribute the bending material to prevent wing ground strikes. To maximize the beneficial influence of the strut upon the wing structure, strut force and spanwise position of the wing-strut intersection are optimized by the MDO code for the 2.5g maneuver load case.

In order to attain acceptable aerodynamic characteristics of the strut, an airfoil cross section is considered. The strut is designed the way that it will not carry aerodynamic forces during the cruise condition.

### **Structural Assumptions**

Preliminary studies have shown buckling of the strut under the -1.0g load condition to be the critical structural design requirement in the single-strut configuration, resulting in high strut weights [3]. To address this issue, an innovative design strategy employs a telescoping sleeve mechanism to allow the strut to be inactive during negative g maneuvers and active during positive g maneuvers. Thus, during the -1.0g maneuver, the wing acts like a cantilever beam and for the positive g maneuvers, the wing is a strut-braced beam.

Even more wing weight reduction can be obtained by optimizing the strut force and wing-strut junction location. For a typical optimum single-strut design, this means that the strut would first engage in tension at some positive load factor. This can be achieved by providing a slack in the wing-strut mechanism. The optimum strut force at 2.5g is different from the strut force that would be obtained at 2.5g if the strut were engaged for all positive values of the load factor.

The slack load factor is defined as the load factor at which the strut initially engages. It is important to have the slack load factor always positive, otherwise the strut would be pre-loaded at the jig shape of the wing to achieve the optimum strut force. To prevent

the strut from engaging and disengaging during cruise due to gust loads, the upper limit for the slack load factor is set to 0.8 during the optimization.

### Double Plate Model

For calculating the wing-bending weight of single strut configurations, a piecewise linear beam model, representing the wing structure as an idealized double plate model, was used first (Figure 1).

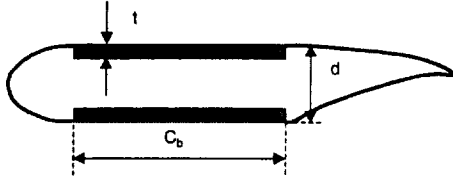


Figure 1: Double plate model for bending weight calculation

This model is made of upper and lower skin panels, which are assumed to carry the bending moment. The double-plate model offers the possibility to extract the material thickness distribution by a closed-form equation. The cross-sectional moment of inertia of the wing box can be expressed as:

$$I(y) = \frac{t(y)c_b(y)d^2(y)}{2} \quad (1)$$

where  $t(y)$  is the wing skin thickness,  $c_b(y)$  is the wing box chord, and  $d(y)$  is the wing airfoil thickness. To obtain the bending material weight, the corresponding bending stress in the wing is calculated from:

$$\sigma_{\max} = \frac{M(y)d(y)}{2I(y)} \quad (2)$$

where  $\sigma_{\max}$  denotes the maximum stress,  $M(y)$  is the bending moment of the wing, and  $I(y)$  denotes the cross-sectional moment of inertia.

If the wing is designed according to the fully-stressed criterion, the allowable stress  $\sigma_{all}$  can be substituted into Eq. (2) for  $\sigma_{\max}$ . Substituting  $I(y)$  into equation (2), the wing panel thickness can be specified as:

$$t(y) = \frac{|M(y)|}{c_b(y)d(y)\sigma_{all}} \quad (3)$$

### Wing Bending Moment Distribution

The local lift distribution can be written as:

$$q_i(y) = \left[ \frac{(y - y_{i+1})}{(y_i - y_{i+1})} \alpha_i + \frac{(y - y_i)}{(y_{i+1} - y_i)} \beta_i \right] \quad (4)$$

where  $q_i(y)$  denotes the local lift distribution for element  $i$ ,  $\alpha_i$  and  $\beta_i$  denote the lift coefficients at nodes  $i$  and  $i+1$ , and  $y_i$  and  $y_{i+1}$  denote the node coordinates in the  $y$ -direction. The piecewise model in global coordinates is shown in Figure 2.

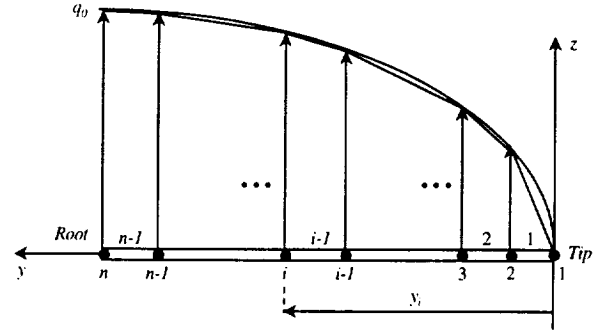


Figure 2: Piecewise aerodynamic loads representation

The shear force and moment equations are obtained from the spanwise lift distribution by applying the well-known beam equations. Since for the  $-1.0g$  load case, the strut is not active, the load distribution is identical to the one obtained for a cantilever wing. Therefore, it is not displayed here. For the  $2.5g$  maneuver case, the strut is active, adding an additional shear force and bending moment to the wing.

As a result, the shear force develops to:

$$V(y) = W_e u[y - (b/2 - y_e)] + F_{sv} u[y - (b/2 - s)] - \int_0^y q(y) dy \quad (5)$$

Consequently, the bending moment on the strut-braced wing is obtained by integration of the shear force along the span:

$$M(y) = -V(y)y - W_e e u[y - (b/2 - y_e)] + F_{sv} (b/2 - s) u[y - (b/2 - s)] - \int_0^y y q(y) dy + W_e (b/2 - y_e) u[y - (b/2 - y_e)] + F_{sh} L_{off} u[y - (b/2 - s)] \quad (6)$$

In Eq. (6)  $u(y)$  is a unit step function defined as:

$$u(y) = \begin{cases} 0 & \text{if } y < 0 \\ 1 & \text{if } y \geq 0 \end{cases} \quad (7)$$

The structural boundary conditions are:

$$\begin{aligned} \theta(b/2) &= 0 \\ w(b/2) &= 0 \end{aligned} \quad (8a, b)$$

The calculated panel thickness is modified by the results obtained from the tip displacement constraint optimization. Therefore, the bending material weight of the half-wing is:

$$W_{wb} = 2 \int_0^{b_s/2} t(y) c_b(y) \rho dy \quad (9)$$

where  $b_s$  is the structural span with  $b_s = b/\cos \Lambda$ .

### Vertical Strut Offset

To reduce the wing/strut interference drag, a vertical offset between strut and wing is implemented. The vertical offset member is designed for a combined bending/tension loading. In this context, the horizontal component of the strut force is of special concern (Fig.6). Since this horizontal force results in a considerable bending load on the offset piece, its weight increases dramatically with increasing strut force and offset length.

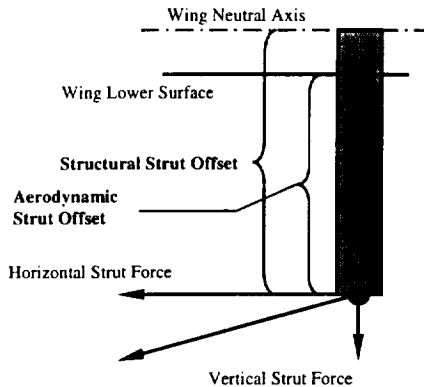


**Figure 3:** Vertical strut offset and applied loads

As a result, it is imperative to employ MDO tools to obtain optimum values for vertical offset, strut force, and spanwise wing/strut breakpoint. This way, it is possible to trade off two contrary design requirements: (i) reduced offset length to reduce strut loading, (ii) increased offset length to reduce wing/strut interference drag. After a complete design optimization with the vertical strut offset as an active design variable, the influence of the offset weight on the total strut weight becomes comparably small. For the wing bending weight and TOGW it is almost immaterial.

### Hexagonal Wing-Box Model

Although the double plate model renders very accurate estimates for the wing bending material weight, it is not suitable for calculation of the wing-box torsional stiffness. This torsional stiffness becomes essential when calculating wing twist and flexible wing

spanload, as well as for the incorporation of aeroelastic constraints into the MDO optimization.

Therefore, a hexagonal wing-box model was implemented into the wing weight calculation module. This model was provided by Lockheed

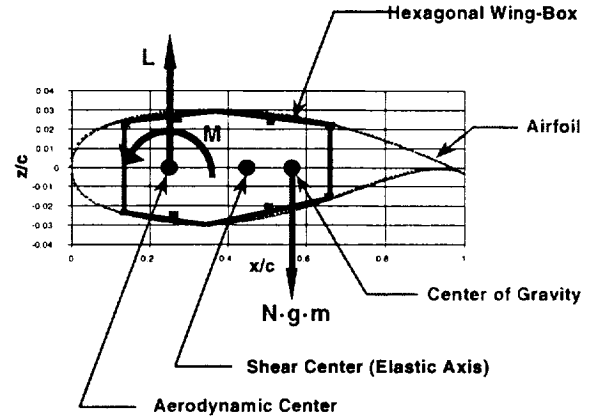


**Figure 4:** Hexagonal wing-box and applied sectional forces and moments

Martin Aeronautical Systems in Marietta, Georgia. Based upon Lockheed Martin's experience in wing sizing, the wing-box geometry varies in the spanwise direction with optimized area and thickness ratios for spar webs, spar caps, stringers, and skins. By keeping these ratios fixed, it is still possible to reduce all geometric data of the wing-box to one independent thickness which is allowed to vary in the spanwise direction. Therefore, despite the complexity of the geometry, a closed solution for the material thickness can still be found by employing the piecewise linear load representation.

In contrast to the double plate model, the hexagonal wing-box allows computation of bending and torsional stiffness with a high degree of accuracy. Furthermore, minimum gauges and maximum stress cutoffs can be accurately applied.

### Aerodynamic Modeling

The aerodynamic loads are calculated based on the well-accepted vortex lattice concept (VLM). For this purpose, a linearized transonic VLM code was developed. To account for compressibility effects, the airflow density is corrected according to the freestream Mach number using a linear approximation. Although not capable of transonic shock predictions, this modification allows very accurate calculations of local lift coefficients. To take into account the spanwise variation of the sectional

pitch and dihedral, as well as the chordwise variation of the airfoil camber surface, the flow tangency boundary condition is formulated as:

$$U_{\infty} \sin(\alpha - \delta) \cos \gamma = w_{ab} \cos \gamma \cos \delta + v_{ab} \sin \gamma \cos \delta - u_{ab} \cos \gamma \sin \delta \quad (10)$$

where  $\alpha$ ,  $\gamma$  and  $\delta$  are the angle of attack, dihedral, and slope of the mean camber line, respectively, for each point on the curved surface. The induced velocities  $u_{ab}$ ,  $v_{ab}$  and  $w_{ab}$  represent the backwash, sidewash and downwash velocities, respectively, acting on any arbitrary point C ( $x_c, y_c, z_c$ ) of the lifting surface due to a bound vortex AB having the vortex strength  $\Gamma$  and the end points A ( $x_a, y_a, z_a$ ) and B ( $x_b, y_b, z_b$ ) (see Appendix A).

The developed lifting surface aerodynamic code has been validated with several well documented test cases, among them a delta wing of aspect ratio  $AR = 2$ , as well as the unswept and swept wings investigated by Weissinger (Figure 5).

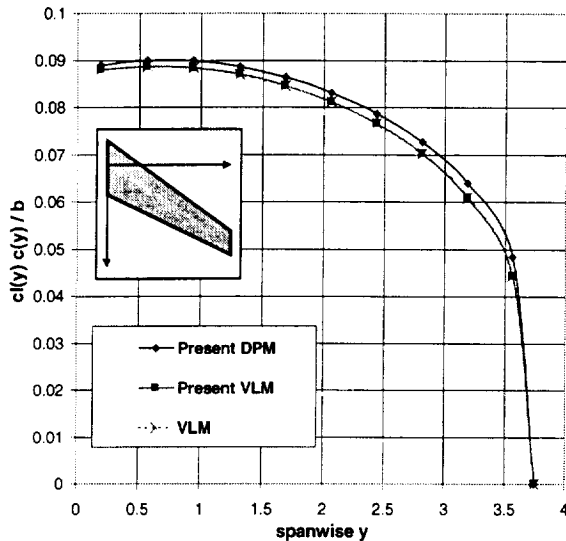


**Figure 5:** Validation of the VLM for Weissinger's swept wing ( $AR = 5$ , taper ratio = 0.5,  $\Lambda = 35^\circ$ , angle of attack =  $5.8^\circ$ )

### **Flexible Wing Sizing**

For accurate wing sizing, the wing has been subdivided into 81 structural nodes representing the spanwise grid points for the application of the piecewise linear loads. To account for increasing gradients in the spanload towards the wing tip, cosine spacing is being used. The aerodynamic lifting surface

features 40 spanwise and 5 chordwise vortex panels distributed equally along the wing span.

In a first step, the wing deformation including sectional twist angle, dihedral (bending slope) and deflection, is calculated from the initial wing spanload. Since the aircraft wing is being optimized for minimum induced drag by the MDO code, this initial spanload usually is close to an elliptical one.

To obtain an elliptical lift distribution during cruise, the wing is being pre-twisted and jig twisted. The pre-twist of the wing planform is calculated using Lamar's design program LAMDES [13]. Since, for a swept wing, the sectional streamwise angle of attack is a combination of twist angle and bending slope, the wing bending deformation significantly influences the aerodynamic effectiveness of the lifting surface. Therefore in order to achieve the desired twist distribution of the wing during cruise, the wing is jig twisted to account for the changes in the local twist due to the bending deformation.

Gimmestad from the Boeing Company showed that consideration of the jig twist for wing sizing of the B-52 resulted in a 10% reduction in the design loads [14]. Therefore, considering the jig twist during preliminary design may result in significant structural weight savings. This holds even more true for the present case where an MDO approach allows weight savings in one component to carry through the overall design of the respective aircraft configuration. In the present code, the jig twist is calculated from the actual wing deformation by subtracting the bending slope from the structural twist of the wing-box.

In the following iteration procedure, the lift distribution is recalculated according to the actual wing deformation, yielding a new (flexible) spanload. Considering the new spanload, all structural wing parameters like bending stiffness, torsional stiffness, and wing weight are recalculated and then again used for computation of the flexible spanload. The wing bending weight is calculated using the panel thickness results or hexagonal wing-box cross sections from the piecewise linear beam model for the different load cases. The overall panel thickness distribution of the wing is obtained by considering the highest value of the panel thickness or cross section at each spanwise position (envelope) [8]. To sustain the total lift for the respective load cases, the total aircraft incidence is recalculated after each iteration step thus ensuring the correct lift for in-flight maneuvers.

The total wing weight, i.e. including the secondary structure like ribs, flaps etc. is calculated using the FLOPS equations [12]. For this purpose, the bending material weight in FLOPS is being replaced by the bending material weight obtained from the present model.

### Validation

To check the integrity of the results, the structural analysis code has been validated using available data for the 747-100. The bending material weight computed from the piecewise linear load model is compared with the bending material weights given by Torenbeek [15] and FLOPS [12]. **Figure 6** highlights the good agreement of both the double plate model and the hexagonal wing-box model with the actual 747-100 weights for the assumption of an elliptical spanload, i.e. a rigid wing model. However, only the hexagonal model allows computation of the wing-box torsional stiffness, thus enabling one to consider the influence of pre-twist, jig twist, and flexible load distribution.

As it can be seen, application of the flexible wing weight calculation procedure as described above can result in significant weight savings for a 747-100 configuration. Interestingly, this potential has already

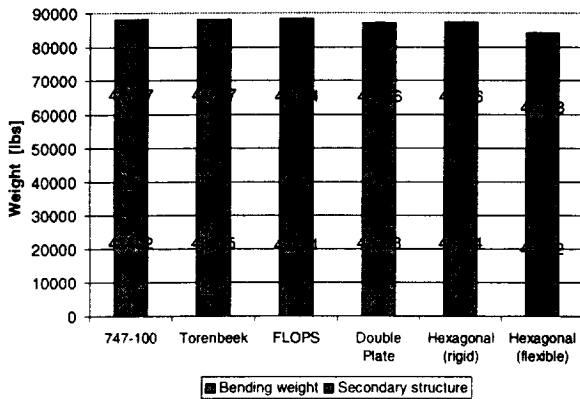


**Figure 6:** Comparison of wing bending material weights and total wing weights for the 747-100

been demonstrated with a flying derivative of this airplane, namely the 747-400.

The bending weight convergence history for this configuration is depicted in **Figure 7**. The structural wing weight is rapidly converging to its final value, exhibiting only small variations after the first iteration step. The reason for this behavior is the relatively high torsional stiffness of this wing-box. Therefore, the

main effect of considering the flexible wing load is due to the recalculation of the bending deformation after the first step and the resulting reduction in the sectional angle of attack (wash-out). This high torsional stiffness is further manifested by the fact

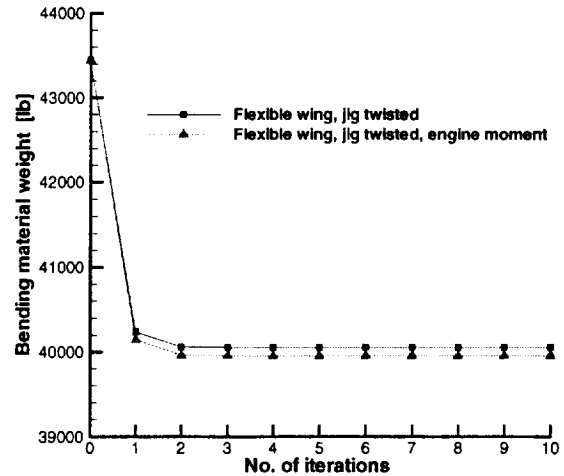


**Figure 7:** Bending material weight convergence history for a 747-100 type wing

that the influence of the engine twist moments is very small, as it can also be seen from **Figure 7**.

The passive load alleviation due to the wash-out effect results in an inboard shifting of the lift loads and therefore reduced bending moments on the outboard sections of the wing. Although the wing structure is resized after each iteration step, the flexible wing spanload rapidly converges to its final

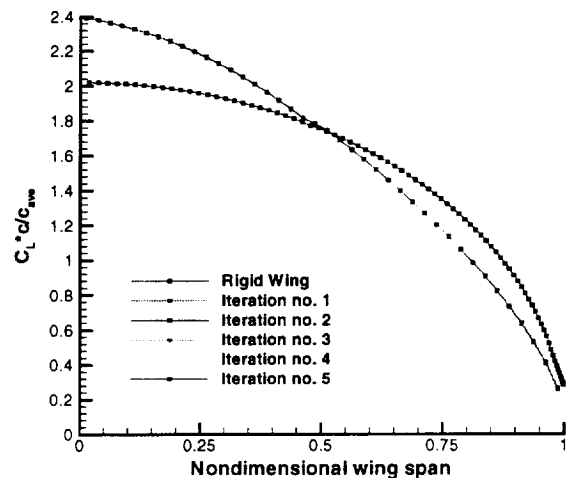


**Figure 8:** Spanload convergence for the 747-100 type flexible wing

distribution (Figure 8). The wing deformation calculated for a 2.5g maneuver for such an optimized wing structure is depicted in Figure 9.

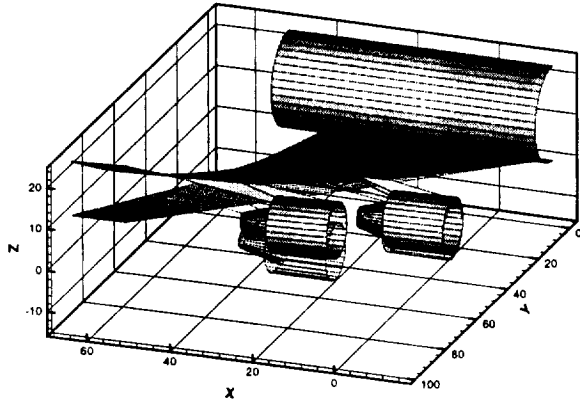


Figure 9: Bending Deformation of the 747-100 type wing configuration

### Strut-Braced Wing Configuration

The strut-braced wing aircraft is obtained from an MDO process as it has been described in [3] and [8]. For the optimization, the aircraft configuration is parameterized into 19 design variables.

Realization of a successful design requires a tight coupling of several disciplines to exploit the synergism in the strut-braced wing concept. Therefore, a multidisciplinary approach is essential. The multidisciplinary team is broken down into aerodynamics, structures, and a detailed investigation of interference drag. The aerodynamic analysis consists of simple models for induced drag, parasite drag, and interference drag. The interference drag model is based on computational fluid dynamics (CFD) analyses of various wing-strut intersection flows. A performance routine is used to evaluate the design constraints and the objective function, TOGW. All these analyses are linked together, and the

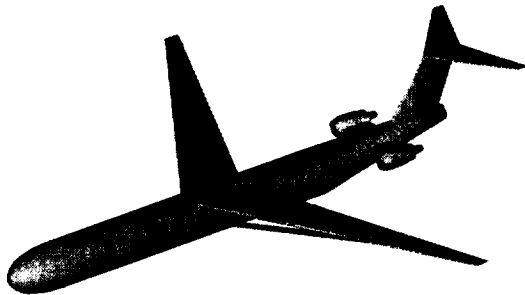


Figure 10: SBW with Fuselage-Mounted Engines

performance of the strut-braced wing is optimized with the Design Optimization package DOT [16].

Using a typical long range mission profile (cruise Mach number 0.85, range 7500Nmi, initial cruise altitude >31,000ft, 325 passengers) the results indicate an overall increase in performance of the strut-braced wing configuration compared to its cantilever counterpart [8]. Figure 10 and Table 1 show the details of the investigated aircraft configuration.

Table 1: Strut-braced wing aircraft parameters

Wing halfspan	108.44 ft
Strut breakpoint	74.52 ft
Wing sweep (3/4 chord)	25.98°
Strut sweep (3/4 chord)	19.01°
Aerodynamic strut offset	2.74 ft
Wing root chord	32.31 ft
Wing breakpoint chord	14.76 ft
Wing tip chord	6.77 ft
Strut chord (constant)	6.62 ft
Wing root t/c	13.75%
Breakpoint t/c	7.23%
Wing tip t/c	6.44%
Strut t/c	8.0%
Strut force	215387.1 lb
Engine nacelle diameter	12.54 ft
Fuselage diameter	20.33 ft
Wing flap area	1411.02 ft <sup>2</sup>
Wing reference area	4237.30 ft <sup>2</sup>
Aircraft zero fuel weight	335590 lb
Take-off gross weight	504833 lb

### Numerical Results

#### Flexible Strut-Braced Wing Spanload

The strut-braced wing as described in the previous section has been analyzed with the new module. Figure 11 shows the spanload distribution on the wing for the 2.5g maneuver obtained from the iteration process. As a first step, the wing structure was kept constant. Spanload and wing deformation were converged to their actual distributions. Basically, the strut-braced wing exhibits the same load alleviation behavior as its cantilever counterpart (Figure 11). Due to the upward bending of the wing, lift loads are shifted inboard because of the reduction of the sectional angle of attack on the outboard wing

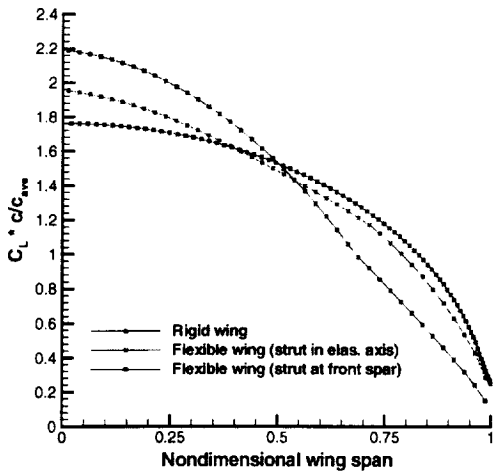


**Figure 11:** Spanload distribution for the strut-braced wing in a 2.5g maneuver

sections (wash-out). For a rigid wing, the spanload for the 2.5g maneuver would be the cruise spanload scaled by the load factor 2.5, i.e. an almost elliptical one.

**Figure 11** also depicts one major advantage of the strut-braced wing from the aeroelastic point of view: a chordwise offset of the strut attachment to the wing-box produces a twist moment acting on the wing. By attaching the strut to the wing-box front spar instead of the wing elastic axis, this moment literally is twisting down the wing leading edge. As a result, even more load is shifted inboard, producing a much higher load alleviation effect than for a conventional wing.

As mentioned before, the aircraft incidence has to be adjusted after each iteration step to sustain the total lift for the respective load factor. As an indicator for

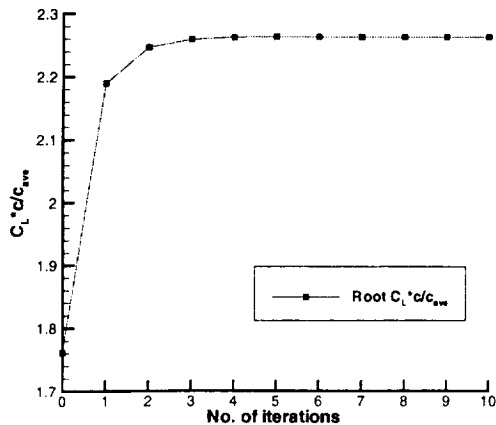


**Figure 12:** Convergence history of the strut-braced wing root lift coefficient

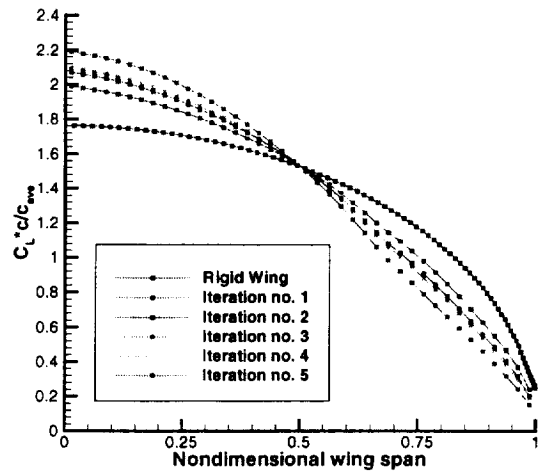


**Figure 13:** Strut-braced wing spanload convergence for the 2.5g maneuver. The strut is attached to the wing-box front spar

the aircraft incidence, **Figure 12** displays the convergence history of the root lift coefficient. The procedure rapidly converges towards the final value, exhibiting a behavior similar to the one observed previously for the cantilever wing aircraft.

### Wing Sizing From Flexible Spanload

Consideration of the actual maneuver spanloads usually results in a significant reduction in the design loads [14]. Since the influence of the strut moment offers even more potential for maneuver load alleviation, the impact of flexible wing sizing may even be higher than for the cantilever wing. As a next step, the wing structure has been resized according to the actual spanload distribution after each iteration

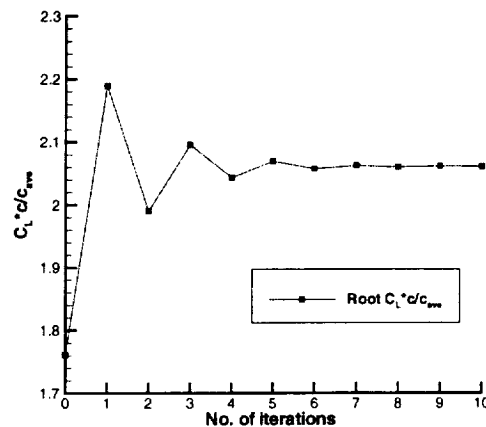


**Figure 14:** Root lift coefficient convergence for the strut-braced wing in a 2.5g maneuver. The strut is attached to wing-box front spar

step. **Figure 13** depicts the spanload distributions for the first five iteration steps and **Figure 14** displays the convergence history of the root lift coefficient. Due to the structural resizing, the convergence of spanload and aircraft incidence becomes slower.

Weight calculation from the flexible design loads reveals the significant influence of the strut moment on maneuver load alleviation and wing weight. **Figure 15** depicts the convergence history of the wing bending material weight for three different strut attachments: at the wing-box front spar, in the wing elastic axis, and at the wing-box rear spar. Compared to the rigid wing weight, sizing the wing using the actual design loads leads to lower weights for all three cases. Nevertheless, it becomes obvious that employment of the strut moment is an important design factor.

It is important to note that an identical wing featuring a thin airfoil would suffer from significant weight penalties if designed without a strut. **Figure 15** indicates a 43% weight penalty for the rigid wing sizing and a 29% weight penalty for the flexible design loads in such a case. Presently, the MDO optimization

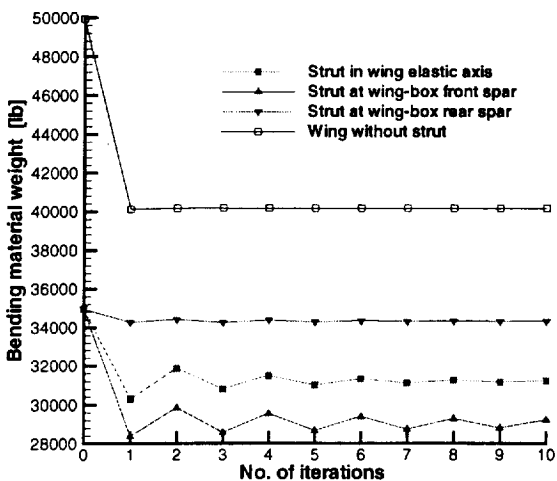


**Figure 15:** Bending material weight convergence for different strut attachments

considers the rigid lift distribution for wing sizing. Therefore, runtime application of flexible spanloads may result in an optimum wing configuration different from the investigated one.

**Figure 16** highlights the influence of the chordwise strut position on the wing bending material weight. The bending material weight increases if the strut is attached to the rear parts of the wing-box. By moving the strut backward in the chordwise direction, the influence of the strut moment is inverted, i.e. it literally is pulling the leading edge upward. As a

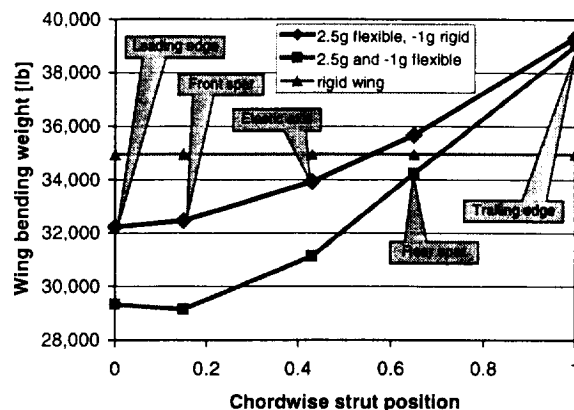


**Figure 16:** Influence of the chordwise strut position on the wing bending material weight

result, lift loads are shifted outboard instead of inboard. This special way of “load aggravation” leads to higher bending moments and higher bending material weights (**Figure 17**).

The chordwise strut position and the resulting twist moment not only influence spanload and structural wing weight, but also wing bending and twist deformations. For the 2.5g maneuver, the upward bending of the wing significantly decreases by moving the strut towards the leading edge of the wing (**Figure 18**). In the same way, the wing twist is being reduced.

Since the strut is not active during the -1.0g pushover, the downward deflections for this maneuver usually are relatively high. Depending on the chordwise strut position, the wing structure is resized according to the actual design loads.

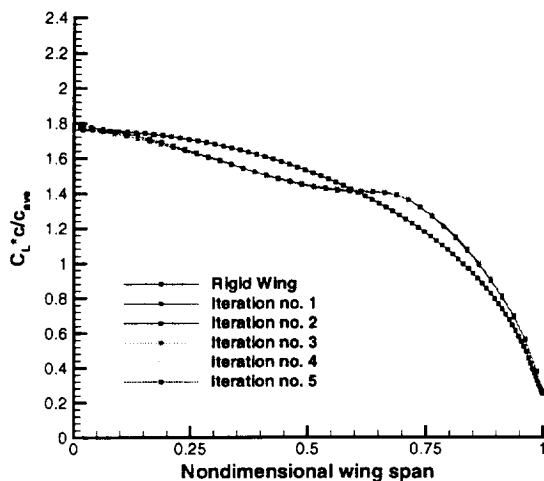


**Figure 17:** Spanload convergence for the 2.5g maneuver. The strut is attached to the wing-box rear spar

Therefore, also for the  $-1.0g$  pushover, the deflections slightly depend on the strut position (**Figure 19**).

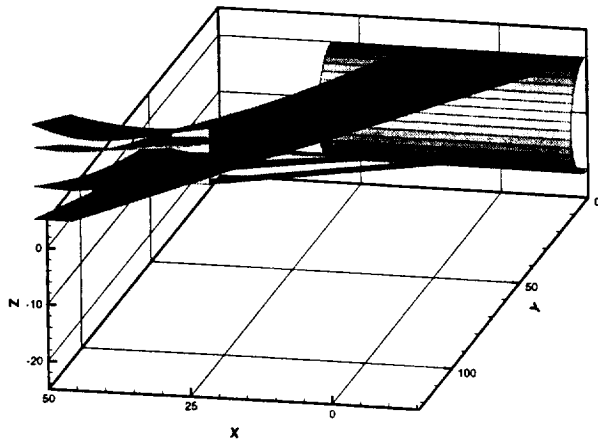


**Figure 18:** Strut-braced wing deformation for the  $2.5g$

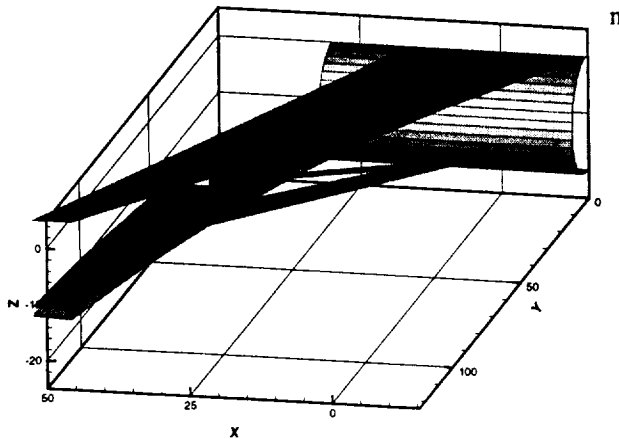


**Figure 19:** Downward deflections for the  $-1.0g$  pushover

### Conclusions

A structural model for wing sizing and weight calculation of a strut-braced wing has been developed. To consider the influence of the actual design loads on the flexible wing, static aeroelastic deformations and flexible wing spanloads have been calculated. Validation of the module with an existing aircraft wing and comparison with results from other sources showed very good agreement with the present model.

The calculations revealed the significant influence of the strut on the bending material weight of the wing. The use of a strut enables one to design a wing with thin airfoils without weight penalty. Designing an identical thin airfoil wing without strut would result in a 40% increase in wing weight.

The strut also influences spanload distributions, wing deformations. Weight savings are not only possible by calculation and iterative resizing of the wing structure according to the actual design loads. Moreover, as an advantage over the cantilever wing, employment of the strut twist moment for further load alleviation leads to increased savings in structural weight.

Ongoing investigations focus on the influence of the strut upon the flutter behavior of the strut-braced wing and on a complete incorporation of the flexible wing sizing routine into the strut-braced wing aircraft design process, i.e. the MDO environment.

### Acknowledgments

This project is funded by NASA Langley Grant NAG 1-1852. Part of the work was done under subcontract from Lockheed Martin Aeronautical Systems in Marietta, Georgia. The authors would like to thank Bob Olliffe from Lockheed Martin Aeronautical Systems for the valuable input and discussions concerning the structural data for the hexagonal wing-box model. Finally, the authors want to thank all their colleagues from the strut-braced wing team for their active contributions throughout the project.

### References

- [1] Pfenninger, W., "Design Considerations of Large Subsonic Long Range Transport Airplanes with Low Drag Boundary Layer Suction," Northrop Aircraft, Inc., Report NAI-54-800 (BLC-67), November 1954.
- [2] Joslin, R.D., "Aircraft Laminar Flow Control," *Annual Review of Fluid Mechanics*, Annual Reviews Inc., Vol. 30, pp. 1-29, Palo Alto, CA, 1998.
- [3] Grasmeyer, J.M., Naghshineh-Pour, A.H., Tetrault, P.A., Grossman, B., Haftka, R.T., Kapania, R.K., Mason, and W.H., Schetz, "Multidisciplinary Design Optimization of a Strut-Braced Wing Aircraft with Tip-Mounted Engines," MAD Center Report 98-01-01, Virginia Tech, January 1998.
- [4] Kulfan, R.M., and Vachal, J.D., "Wing Planform Geometry Effects on Large Subsonic Military Transport Airplanes," Boeing Commercial Airplane Company, AFFDL-TR-78-16, February 1978.
- [5] Park, H. P., "The Effect on Block Fuel Consumption of a Strutted vs. Cantilever Wing for a Short Haul Transport Including Strut Aeroelastic Considerations," AIAA-78-1454-CP, Los Angeles, California, Aug. 21-23, 1978.

[6] Turriziani, R.V., Lovell, W.A., Martin, G.L., Price, J.E., Swanson, E.E., and Washburn, G.F., "Preliminary Design Characteristics of a Subsonic Business Jet Concept Employing an Aspect Ratio 25 Strut Braced Wing," NASA CR-159361, October 1980.

[7] Grasmeyer, J.M., "Multidisciplinary Design Optimization of a Strut-Braced Wing Aircraft," MS Thesis, Virginia Tech, April 1998.

[8] Gern, F.H., Gundlach, J.F., Ko, A., Naghshineh-Pour, A., Sulaeman, E., Tetrault, P.-A., Grossman, B., Kapania, R.K., Mason, W.H., J.A. Schetz, and Haftka, R.T., "Multidisciplinary Design Optimization of a Transonic Commercial Transport with a Strut-Braced Wing," 1999 World Aviation Congress, 99WAC-30, San Francisco, CA, Oct. 19-21, 1999

[9] Grossman, B., Strauch, G.J., Eppard, W.M., Gurdal, Z., and Haftka, R.T., "Integrated Aerodynamic/Structural Design of a Sailplane Wing," AIAA-86-2623, Dayton, Ohio, October 20-22, 1986.

[10] Giunta, A.A., Balabanov, V., Haim, D., Grossman, B., Mason, W.H., Watson, L.T., and Haftka, R.T., "Multidisciplinary Optimization of a Supersonic Transport Using Design of Experiments Theory and Response Surface Modeling," The Aeronautical Journal, pp. 347-356, October 1997.

[11] Hutchison, M.G., Unger, E.R., Mason, W.H., Grossman, B., Haftka, R.T., "Variable Complexity Aerodynamic Optimization of a High Speed Civil Transport Wing," Journal of Aircraft, Vol. 31, No. 1, pp. 110-116, 1994.

[12] McCullers, L.A., *FLOPS User's Guide, Release 5.81*, NASA Langley Research Center.

[13] Lamar, J.E., "A Vortex Lattice Method for the Mean Camber Shapes of Trimmed Non-Coplanar Planforms with Minimum Vortex Drag," NASA TN D-8090, June, 1976

[14] Gimmestad, D., "An Aeroelastic Optimization Procedure for Composite High Aspect Ratio Wings," AIAA Paper No. 79-0726, April, 1979

[15] Torenbeek, E., "Development and Application of a Comprehensive, Design Sensitive Weight Prediction Method for Wing Structures of Transport Category Aircraft," Delft University of Technology, Report LR-693, Sept. 1992.

[16] Vanderplaats Research & Development, Inc., *DOT User's Manual*, Version 4.20, Colorado Springs, CO, 1995.

[17] Bertin, J.J., Smith, L.L., *Aerodynamics for Engineers*, 2<sup>nd</sup> Ed., Prentice Hall, Englewood Cliffs, 1989

[18] Katz, J., Plotkin, A., *Low-Speed Aerodynamics*, McGraw-Hill, New York, 1991

## Appendix: Vortex Lattice Formulation

Using the Helmholtz method to derive the vortex line downwash and with

$$\beta = \sqrt{1 - M_\infty^2}, \quad (11)$$

it can be shown that the induced velocities develop into the following equations:

Downwash:

$$w_{ab} \left( \frac{\Gamma}{4\pi} \right)^{-1} = \quad (12)$$

$$\begin{aligned} & \frac{x_{ac}y_{ab} - x_{ab}y_{ac}}{(x_{ac}y_{ab} - x_{ab}y_{ac}) + (x_{ac}z_{ab} - x_{ab}z_{ac}) + \beta^2(y_{ac}z_{ab} - y_{ab}z_{ac})} \times \\ & \left\{ \frac{x_{bc}x_{ab} + \beta^2(y_{bc}y_{ab} + z_{ab}z_{bc})}{\sqrt{x_{bc}^2 + \beta^2(y_{bc}^2 + z_{bc}^2)}} - \frac{x_{ac}x_{ab} + \beta^2(y_{ac}y_{ab} + z_{ab}z_{ac})}{\sqrt{x_{ac}^2 + \beta^2(y_{ac}^2 + z_{ac}^2)}} \right\} \\ & + \frac{y_{ac}}{y_{ac}^2 + z_{ac}^2} \left( 1 - \frac{x_{ac}}{\sqrt{x_{ac}^2 + \beta^2(y_{ac}^2 + z_{ac}^2)}} \right) \\ & + \frac{y_{bc}}{y_{bc}^2 + z_{bc}^2} \left( 1 - \frac{x_{bc}}{\sqrt{x_{bc}^2 + \beta^2(y_{bc}^2 + z_{bc}^2)}} \right) \end{aligned}$$

Note that for  $M_\infty = 0$ ,  $z = 0$ , and  $\gamma = 0$ , Eq. (12) reduces to the formula used by Bertin and Smith [17].

Backwash:

$$u_{ab} \left( \frac{\Gamma}{4\pi} \right)^{-1} = \quad (13)$$

$$\begin{aligned} & \frac{-y_{ac}z_{ab} + y_{ab}z_{ac}}{(x_{ac}y_{ab} - x_{ab}y_{ac}) + (x_{ac}z_{ab} - x_{ab}z_{ac}) + \beta^2(y_{ac}z_{ab} - y_{ab}z_{ac})} \times \\ & \left\{ \frac{x_{bc}x_{ab} + \beta^2(y_{bc}y_{ab} + z_{ab}z_{bc})}{\sqrt{x_{bc}^2 + \beta^2(y_{bc}^2 + z_{bc}^2)}} - \frac{x_{ac}x_{ab} + \beta^2(y_{ac}y_{ab} + z_{ab}z_{ac})}{\sqrt{x_{ac}^2 + \beta^2(y_{ac}^2 + z_{ac}^2)}} \right\} \end{aligned}$$

Sidewash:

$$v_{ab} \left( \frac{\Gamma}{4\pi} \right)^{-1} = \quad (14)$$

$$\begin{aligned} & \frac{-x_{ac}z_{ab} + x_{ab}z_{ac}}{(x_{ac}y_{ab} - x_{ab}y_{ac}) + (x_{ac}z_{ab} - x_{ab}z_{ac}) + \beta^2(y_{ac}z_{ab} - y_{ab}z_{ac})} \times \\ & \left\{ \frac{x_{bc}x_{ab} + \beta^2(y_{bc}y_{ab} + z_{ab}z_{bc})}{\sqrt{x_{bc}^2 + \beta^2(y_{bc}^2 + z_{bc}^2)}} - \frac{x_{ac}x_{ab} + \beta^2(y_{ac}y_{ab} + z_{ab}z_{ac})}{\sqrt{x_{ac}^2 + \beta^2(y_{ac}^2 + z_{ac}^2)}} \right\} \\ & + \frac{z_{ac}}{y_{ac}^2 + z_{ac}^2} \left( 1 - \frac{x_{ac}}{\sqrt{x_{ac}^2 + \beta^2(y_{ac}^2 + z_{ac}^2)}} \right) \\ & + \frac{z_{bc}}{y_{bc}^2 + z_{bc}^2} \left( 1 - \frac{x_{bc}}{\sqrt{x_{bc}^2 + \beta^2(y_{bc}^2 + z_{bc}^2)}} \right) \end{aligned}$$

Note that for  $M_\infty = 0$ , Eqs. (12) to (14) reduce to the formulae used by Plotkin and Katz [18].